Inorg. Chem. **2005**, *44*, 8293−8305

Inorganic Chemistry
Article

Bimodal System (Luminophore and Paramagnetic Contrastophore) Derived from Ln(III) Complexes Based on a Bipyridine-Containing Macrocyclic Ligand

Isabelle Nasso,[†] Chantal Galaup,[†] Fabien Havas,[†] Pierre Tisnès,[†] Claude Picard,*[,†] Sophie Laurent,[‡] Luce Vander Elst,[‡] and Robert N. Muller*[,‡]

Laboratoire de Synthèse et Physicochimie de Molécules d'Intérêt Biologique, CNRS UMR 5068, Université Paul Sabatier, 118 route de Narbonne, 31062 Toulouse cedex 04, France, and Department of Organic and Biomedical Chemistry, NMR and Molecular Imaging Laboratory, University of Mons-Hainaut, B-7000 Mons, Belgium

Received May 13, 2005

The synthesis of a new 15-membered polyaza-macrocyclic ligand $\mathbf{L^3H_3}$, which is based on a 2,2′-bipyridine moiety and a diethylenetriaminetriacetic acid core, is reported. The lanthanide chelates of this octadentate ligand were programmed for bimodal probes, luminescent agents (Sm, Eu, Tb, Dy), and magnetic resonance imaging agents (Gd^{3+}). The neutral 1:1 complexes with these Ln^{3+} ions were prepared and studied in aqueous solution by luminescence and NMR techniques. The main photophysical characteristics of these complexes (i.e., the absorption and luminescence spectra, the metal-centered lifetimes, and the overall luminescence yields, Φ) were measured. In addition, the role played by nonradiative pathways (vibrational energy transfer involving coordinated water molecules, involvement of ligand-to-metal charge-transfer excited states, or metal → ligand back transfer) is discussed. The $\mathbf{L^3 \cdot Eu}$ and $\mathbf{L^3 \cdot Tb}$ complexes show very bright luminescence when photoexcited from the lowest-energy absorption band of the bipyridine chromophore. The luminescence quantum yields in an air-equilibrated water solution at room temperature are 0.10 and 0.21, respectively, despite the presence of one water molecule in the first coordination sphere of the metal ion. NMR data show that $\mathbf{L^3 \cdot Gd}$ contains also one H_2O molecule in the inner sphere. The proton longitudinal relaxivity, r_1, of this complex is 3.4 s^{-1} mM^{-1} (0.47 T, 310 K) and the rotational correlation time, τ_R, is 57 ps (310 K). These values are comparable to those of the clinically used Gd-DTPA. Interestingly, the water exchange rate between the coordination site and the bulk solvent is slow ($\tau_M = 3.5$ μs at 310 K). The presence of water molecules in the second sphere and in rapid exchange with the solvent is discussed. Finally, it was found by luminescence and NMR experiments that these lanthanide complexes are stable versus transmetalation by several cations (especially Ca^{2+} and Zn^{2+}) at physiological pH and have no interaction with blood proteins.

Introduction

Over the past decade, a large effort has been devoted to the rational design and synthesis of organic polydentate ligands capable of forming stable lanthanide complexes in aqueous solutions. These studies have been motivated by the successful applications of Ln^{III} systems in medicine and biology. The paramagnetic Gd^{III} ion is currently used to increase the intrinsic contrast of magnetic resonance images in clinical studies (∼30−40% MRI exams).[1] A new generation of MRI contrast agents (CAs), based on gadolinium complexes, with the ability to target specific tissues and organs[2] or with very high relaxivity[3] is presently being developed. In addition to these clinical CAs, recent reports show the possibility of modulating the relaxivity of a Gd^{III}

* To whom correspondence should be addressed. E-mail: picard@chimie.ups-tlse.fr. Phone: (+33) 05 61 55 62 96. Fax: (+33) 05 61 55 60 11 (C.P.). E-mail: robert.muller@umh.ac.be. Phone/Fax: (+32) 65 37 35 20 (R.N.M.).
† Université Paul Sabatier.
‡ University of Mons-Hainaut.

(1) (a) Merbach, A. E.; Toth, E. In *The Chemistry of Contrast Agents in Medical Magnetic Resonance Imaging*; Wiley: London, 2001. (b) Caravan, P.; Ellison, J. J.; McMurry, T. J.; Lauffer, R. B. *Chem. Rev.* **1999**, *99*, 2293−2352. (c) Aime, S.; Botta, M.; Fasano, M.; Terreno, E. *Chem. Soc. Rev.* **1998**, *27*, 19−29.
(2) Weinmann, H.-J.; Ebert, W.; Misselwitz, B.; Schmitt-Willich, H. *Eur. J. Radiol.* **2003**, *46*, 33−44.

10.1021/ic0507722 CCC: $30.25
Published on Web 10/14/2005

complex according to its biochemical environment.[4] The long luminescence lifetime (ms range) of Eu^{III} and Tb^{III} ions permits easy temporal resolution from the short-lived (ns range) fluorescence background present in biological samples.[5] Consequently, applications of Eu- and Tb-labeled ligands and time-resolved technologies are rapidly growing in the fields of biomedical and biological applications.[6−8]

If a high kinetic inertness in aqueous solutions is a shared prerequisite for lanthanide complexes used as MRI contrast agents or luminescent bioprobes, it should be noted that the denticity requirement for the chelator is not the same in these two systems. The Gd^{III} complex should have at least one vacant inner-sphere coordination site for water ligand exchange to enhance the water proton-relaxation rates. In contrast, the Eu^{III} or Tb^{III} ions should be fully shielded from surrounding H_2O molecules which contribute to nonradiative de-excitation and a reduced quantum yield for lanthanide luminescence. Moreover to achieve strong luminescence, the ligand should act as an "antenna", with a large absorption cross section at a suitable excitation wavelength and an efficient energy transfer to metal excitation state. The main research effort for Gd^{3+}-based MRI agents and photoactive Eu^{3+} and Tb^{3+} complexes has been directed toward two main classes of ligands: aminopolycarboxylic open-chain ligands and DOTA-type macrocyclic derivatives.[1,9]

Our interest in the development of Gd-based ligands[10] or Eu- and Tb-based tags[11] for use as contrast agents for functional MRI or as luminescent biolabels had led us to investigate a system that forms both efficient luminescent Eu and Tb complexes and Gd relaxation agents. Such magnetic and luminescent probes, based on identical structures, could offer the opportunity to directly correlate in vitro (time-resolved luminescence microscopy) and in vivo (MRI) imaging studies.[12] Sherry and co-workers[13] examined some of the chemical and magnetic properties of lanthanide complexes derived from a 12-membered tetraaza macrocyclic acetate ligand containing pyridine (PCTA[12],[14] ligand $\mathbf{L^1H_3}$, Chart 1). The measured relaxivity for the corresponding Gd^{III} complex is quite high (6.9 s^{-1} mM^{-1} at 20 MHz and 25 °C) because of the presence of two water molecules in the inner coordination sphere of the ion.[15] This metal hydration state, associated with a pyridine antenna effect, induce a poor sensitization of the Eu-centered luminescence (absolute quantum yield, Φ, is 0.029).[16] More recently, some of us reported the synthesis and the photophysical properties of an analogous 18-membered macrocycle (tpyCTA[18],[14] ligand $\mathbf{L^2H_3}$, Chart 1) where a terpyridine unit is substituted for the pyridine ring.[17] This chelator induces high kinetic stability of the resulting Ln^{III} complexes in aqueous solutions and displays an excellent antenna effect for both Eu^{III} and Tb^{III} luminescence ($\Phi = 0.18$ and 0.21, respectively). On the other hand, the nonadenticity of this ligand precludes the coordination of a water molecule in the inner sphere of the metal and consequently its Gd^{III} complex cannot be an effective contrast agent.

Chart 1

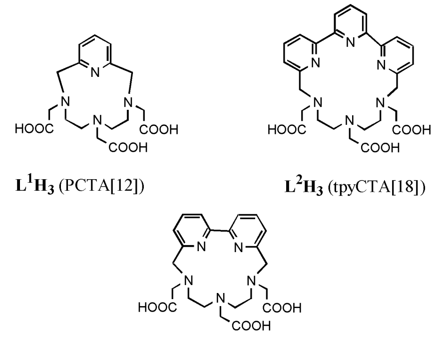

$\mathbf{L^1H_3}$ (PCTA[12]) $\mathbf{L^2H_3}$ (tpyCTA[18]) $\mathbf{L^3H_3}$ (bpyCTA[15])

(3) (a) Fatin-Rouge, N.; Toth, E.; Meuli, R.; Bünzli, J.-C. G. *J. Alloys Compd.* **2004**, *374*, 298−302. (b) Vander Elst, L.; Port, M.; Raynal, I.; Simonot, C.; Muller, R. N. *Eur. J. Inorg. Chem.* **2003**, 2495−2501. (c) Toth, E.; Helm, L.; Kellar, K. E.; Merbach, A. E. *Chem.*−*Eur. J.* **1999**, *5*, 1202−1211. (d) Muller, R. N.; Radüchel, B.; Laurent, S.; Platzek, J.; Piérart, C.; Mareski, P.; Vander Elst, L. *Eur. J. Inorg. Chem.* **1999**, 1949−1955.

(4) (a) Lowe, M. P. *Aust. J. Chem.* **2002**, *55*, 551−556. (b) Meade, T. J.; Taylor, A. K.; Bull, S. R. *Curr. Opin. Neurobiol.* **2003**, *13*, 597−602.

(5) (a) Richardson, F. S. *Chem. Rev.* **1982**, *82*, 541−552. (b) Sammes, P. G.; Yahioglu, G. *Nat. Prod. Rep.* **1996**, *13*, 1−28.

(6) (a) Bünzli, J.-C. G. In *Metal Complexes in Tumor Diagnosis and as Anticancer Agents*; Sigel, A., Sigel, H., Eds.; Metal Ions in Biological Systems, Vol. 42; Marcel Dekker Inc.: New York, 2004; Chapter 2. (b) Motson, G. R.; Fleming, J. S.; Brooker, S. *Adv. Inorg. Chem.* **2004**, *55*, 361−432. (c) Steinkamp, T.; Karst, U. *Anal. Bioanal. Chem.* **2004**, *380*, 24−30. (d) Bazin, H.; Trinquet, E.; Mathis, G. *Rev. Mol. Biotechnol.* **2002**, *82*, 233−250. (e) Hemmilä, I.; Webb, S. *Drug Discovery Today* **1997**, *2*, 373−381. (f) *Bioanalytical Applications of Labeling Technologies*; Hemmila, I., Stahlberg, T., Mottram, P., Eds.; Wallac Oy: Turku, Finland, 1995.

(7) (a) Kolb, A. J.; Burke, J. W.; Mathis, G. In *High Throughput Screening: The Discovery of Bioactive Substances*; Devlin, J. P., Ed.; Marcel Dekker: New York, 1997; pp 345−360. (b) Frias, J. C.; Bobba, G.; Cann, M. J.; Hutchison, C. J.; Parker, D. *Org. Biomol. Chem.* **2003**, *1*, 905−907. (c) Hemmila, I.; Mukkala, V.-M. *Crit. Rev. Clin. Lab. Sci.* **2001**, *38*, 441−519.

(8) (a) Bornhop, D. J.; Griffin, J. M. M.; Goebel, T. S.; Sudduth, M. R.; Bell, B.; Motamedi, M. *Appl. Spectrosc.* **2003**, *57*, 1216−1222. (b) Bornhop, D. J.; Hubbard, D. S.; Houlne, M. P.; Adair, C.; Kiefer, G. E.; Pence, B. C.; Morgan, D. L. *Anal. Chem.* **1999**, *71*, 2607−2615. (c) Hubbard, D. S.; Houlne, M. P.; Kiefer, G. E.; McMillan, K.; Bornhop, D. J. *Bioimaging* **1998**, *6*, 63−70.

(9) (a) Frullano, L.; Rohovec, J.; Peters, J. A.; Geraldes, C. F. G. C. *Top. Curr. Chem.* **2002**, *221*, 25−60. (b) Thunus, L.; Lejeune, R. *Coord. Chem. Rev.* **1999**, *184*, 125−155.

(10) (a) Laurent, S.; Vander Elst, L.; Fu, Y.; Muller, R. N. *Bioconjugate Chem*. **2004**, *15* (1), 99−103. (b) Laurent, S.; Botteman, F.; Vander Elst, L.; Muller, R. N. *Eur. J. Inorg. Chem*. **2004**, 463−468. (c) Laurent, S.; Botteman, F.; Vander Elst, L.; Muller, R. N. *Helv. Chim. Acta* **2004**, *87*, 1077−1089.

(11) (a) Galaup, C.; Couchet, J.-M.; Bedel, S.; Tisnès, P.; Picard, C. *J. Org. Chem.* **2005**, *70*, 2274−2284. (b) Tedeschi, C.; Azéma, J.; Gornitzka, H.; Tisnès, P.; Picard, C. *J. Chem. Soc., Dalton Trans.* **2003**, 1738−1745. (c) Galaup, C.; Azéma, J.; Tisnès, P.; Picard, C.; Ramos, P.; Juanes, O.; Brunet, E.; Rodríguez-Ubis, J. C. *Helv. Chim. Acta* **2002**, *85*, 1613−1625. (d) Galaup, C.; Carrié, M.-C.; Tisnès, P.; Picard, C. *Eur. J. Org. Chem.* **2001**, 2165−2175.

(12) For a recent example, see: Manning, H. C.; Goebel, T.; Thompson, R. C.; Price, R. R.; Lee, H.; Bornhop, D. J. *Bioconjugate Chem.* **2004**, *15*, 1488−1495.

(13) Kim, W. D.; Kiefer, G. E.; Maton, F.; McMillan, K.; Muller, R. N.; Sherry, A. D. *Inorg. Chem.* **1995**, *34*, 2233−2243.

(14) PCTA[12] = 12-membered **p**yridine **c**ontaining a **t**ri**a**za macrocycle triacetate ligand, bpyCTA[15] = 15-membered **b**i**py**ridine **c**ontaining **a** **t**ri**a**za macrocycle triacetate ligand, and tpyCTA[18] = 18-membered **t**er**py**ridine **c**ontaining a **t**ri**a**za macrocycle triacetate ligand.

(15) Aime, S.; Botta, M.; Geninatti Crich, S.; Giovenzana, G. B.; Jommi, G.; Pagliarin, R.; Sisti, M. *Inorg. Chem.* **1997**, *36*, 2992−3000.

(16) Siaugue, J.-M.; Favre-Réguillon, A.; Dioury, F.; Plancque, G.; Foos, J.; Madic, C.; Moulin, C.; Guy, A. *Eur. J. Inorg. Chem.* **2003**, 2834−2838.

(17) Galaup, C.; Couchet, J. M.; Picard, C.; Tisnès, P. *Tetrahedron Lett.* **2001**, *42*, 6275−6278.

Because the 2,2′-bipyridine chromophore is known to act as an efficient photosensitizer antenna to enhance the luminescence of Eu^{III} and Tb^{III}, we have designed a 15-membered macrocycle incorporating this moiety (bpyCTA-[15],[14] ligand $\mathbf{L^3H_3}$, Chart 1). The expected octacoordinating nature of this ligand allows one water molecule to coordinate the metal center since the Eu^{III}, Gd^{III}, and Tb^{III} ions are nonacoordinated species in aqueous solution.[18] We can also notice that the net charge of these complexes is neutral, an important factor to take into account, since positively or negatively charged complexes induce high osmolality and may lead to nonspecific binding in biological media. This could have some benefit in applications.[19] We report herein on (i) the synthesis of this new polydentate ligand, $\mathbf{L^3H_3}$, incorporating five-membered chelate rings, (ii) the luminescence properties of the resulting complexes formed with ions used in fluoroimmunoassays (Ln = Sm, Eu, Tb, Dy), and (iii) the relaxometric properties of the Gd complex. A comprehensive study was also undertaken to gain insight into the parameters which govern the photophysics and relaxation processes in these complexes. Attention is also focused on the resistance (kinetic stability) of these metal probes toward the dissociation and transmetalation processes. Preliminary results from this work have been published previously.[20]

Experimental Section

Synthesis. General Procedures and Starting Materials. 6,6′-Bis(bromomethyl)-2,2′-bipyridine **1**,[11d] 1,4,7-tritosyl-1,4,7-triazaheptane **2**,[21] 1,4,7-triazaheptane-1,4,7-triacetic acid tri-*tert*butyl ester **5**,[11a] and compound **4**[22] were prepared according to literature procedures. Column chromatography was carried out on alumina (Macherel-Nagel, activity IV, 50−200 μm) or C_{18} reverse-phase silica. The HPLC analyses were performed on a Waters Alliance 2690 instrument equipped with a Waters PDA 2996 photodiode array detector. Melting points were determined on a Electrothermal IA9200 apparatus. ^1H and ^{13}C NMR spectra were recorded on Bruker AC250 and Avance 400 spectrometers. IR spectra were determined with a Perkin-Elmer FT-IR 1725x spectrometer. Fast atom bombardment (FAB) and electrospray (ES) mass spectra were obtained on a Nermag R10-10C spectrometer and a Perkin-Elmer SCIEX API 100 spectrometer, respectively. UV spectra were recorded on a Hewlett-Packard 8453 UV−vis spectrometer.

Preparation of Compound 3. A mixture of 1,4,7-tritosyl-1,4,7-triazaheptane **2** (945 mg, 1.67 mmol) and K_2CO_3 (2.31 g, 16.7 mmol) in anhydrous acetonitrile (810 mL) was refluxed for 1h. Then, 6,6′-bis(bromomethyl)-2,2′-bipyridine **1** (600 mg, 1.76 mmol) was added in one portion, and the reaction mixture was refluxed overnight. After the mixture was cooled to room temperature, the insoluble solid was filtered off. The solvent was evaporated under reduced pressure, and the solid residue obtained was washed with methanol and dried under vacuum to give compound **3** (954 mg, 77%). mp: 220 °C dec (lit.[22] mp 215 °C). R_f: 0.43 (silica gel, CH_2Cl_2/MeOH 9/1). ^1H NMR ($CDCl_3$, 250 MHz): δ 2.37 (s, 3H), 2.45 (s, 6H), 3.25 (m, 4H), 3.56 (m, 4H), 4.44 (s, 4H), 7.25 (d, 2H, ^3J = 7.3 Hz), 7.35 (d, 4H, ^3J = 8.5 Hz), 7.43 (d, 2H, ^3J = 7.3 Hz), 7.77 (m, 10H). ^{13}C NMR ($CDCl_3$, 62.5 MHz): δ 21.0, 49.3, 49.9, 55.2, 121.4, 123.8, 127.5, 129.8, 135.4, 135.8, 138.5, 143.4, 143.6, 155.5, 157.4.

Preparation of Compounds 6·Na and 6. Na_2CO_3 (380 mg, 3.59 mmol) was added to a solution of triamine **5** (160 mg, 0.36 mmol) in anhydrous acetonitrile (150 mL). The suspension was refluxed for 1 h 30 min, and then a solution of 6,6′-bis(bromomethyl)-2,2′-bipyridine **1** (123 mg, 0.36 mmol) in anhydrous acetonitrile (20 mL) was added dropwise; the mixture was then stirred and refluxed overnight before filtration. The solvent was evaporated under reduced pressure, and the residue was purified by column chromatography on alumina (99/1 to 90/10 $CHCl_3$/MeOH). The selected fractions were combined, and the solvents were removed under reduced pressure. The oily residue was triturated with diethyl ether to yield a yellow waxy solid, which was isolated by filtration and washed with petroleum ether. The waxy solid was redissolved in boiling toluene (10 mL), and the solution was filtered, yielding **6·Na** as a white solid (34 mg, 12%). The mother liquor was concentrated to dryness to give **6**, as a pale yellow oil (55 mg, 22%). Compound **6·Na**. mp: 127−128 °C. R_f: 0.14 (alumina, $CHCl_3$/MeOH 9/1). FT-IR (KBr): ν_{max} 1732 (C=O). ^1H NMR ($CDCl_3$, 400 MHz): δ 1.27 (s, 9H), 1.48 (s, 18H), 2.14−2.93 (m, 10H), 3.65 (AB sys, 4H, $\Delta\nu$ = 40.0 Hz, ^{AB}J = 16.0 Hz), 4.09 (AB sys, 4H, $\Delta\nu$ = 32.0 Hz, ^{AB}J = 15.2 Hz), 7.36 (d, 2H, ^3J = 7.6 Hz), 7.92 (t, 2H, ^3J = 7.8 Hz), 7.99 (d, 2H, ^3J = 7.8 Hz). ^{13}C NMR ($CDCl_3$, 50 MHz): δ 28.1, 28.2, 47.2, 52.0, 52.3, 58.7, 62.1, 81.7, 82.5, 120.4, 123.6, 138.9, 154.1, 158.1, 169.0, 172.9. MS (ESI$^+$, CH_3CN): m/z 648.1 ([M + Na]$^+$, 100%), 592.2 ([M − C_4H_8 + Na]$^+$, 85%), 536.2 ([M − 2 × C_4H_8 + Na]$^+$, 48%), 480.1 ([M − 3 × C_4H_8 + Na]$^+$, 25%). Anal. Calcd For $C_{34}H_{51}N_5O_6NaBr\cdot 0.5CHCl_3$: C, 52.56; H, 6.58; N, 8.88. Found: C, 52.68; H, 6.44; N, 8.61. Compound **6**. R_f: 0.27 (alumina, $CHCl_3$/MeOH 9/1). FT-IR (KBr): ν_{max} 1729 (C=O). ^1H NMR ($CDCl_3$, 250 MHz): δ 1.42 (s, 9H), 1.46 (s, 18H), 3.08 (m, 8H), 3.33 (s, 6H), 4.07 (s, 4H), 7.18 (d, 2H, ^3J = 7.2 Hz), 7.62 (d, 2H, ^3J = 7.5 Hz), 7.70 (t, 2H, ^3J = 7.7 Hz). ^{13}C NMR ($CDCl_3$, 50 MHz): δ 28.2, 51.0, 52.3, 57.1, 57.6, 58.4, 80.7, 81.0, 119.9, 122.9, 136.9, 156.2, 158.5, 170.8. MS (ESI$^+$, CH_3CN): m/z 648.4 ([M + Na]$^+$, 100%), 592.2 ([M − C_4H_8 + Na]$^+$, 40%), 536.2 ([M − 2 × C_4H_8 + Na]$^+$, 17%), 480.1 ([M − 3 × C_4H_8 + Na]$^+$, 10%). Anal. Calcd for $C_{34}H_{51}N_5O_6\cdot 0.5CHCl_3$: C, 60.45; H, 7.57; N, 10.22. Found: C, 60.45; H, 7.71; N, 9.95.

Preparation of Ligand $\mathbf{L^3H_3}$. Triester **6** or **6·Na** (0.11 mmol) was dissolved in a mixture of trifluoroacetic acid/dichoromethane (1/1, 10 mL), and the solution was stirred for 24 h at room temperature. After the solvent evaporated under reduced pressure, the crude mixture was chromatographed on C_{18} reverse-phase silica using 0.1% TFA in H_2O with a gradient of CH_3CN (2 to 10%) as the mobile phase. The desired triacid was obtained as a colorless oil (80−85% yield). t_R: 4.5 min (analytical HPLC; column, CC70−3MN C18 HD 5 μm; eluent, (H_2O, TFA 0.1%)/MeOH 95/5; flow rate, 0.6 mL/min). FT-IR (KBR): ν_{max} 1687 (C=O). UV−vis (HEPES buffer, pH 7.3): λ (ϵ) 246 (7550), 301 (10025), 313 (8025). ^1H NMR (D_2O, 250 MHz): δ 3.43−3.50 (m, 10H), 3.84 (s, 4H), 4.52 (s, 4H), 7.68 (d, 2H, ^3J = 7.5 Hz), 8.25 (t, 2H, ^3J = 7.5 Hz),

(18) Bünzli, J.-C. G. In *Lanthanides, Probes in Life, Chemical and Earth Sciences*; Choppin, G. R., Bünzli, J.-C. G., Eds.; Elsevier: Amsterdam, 1989; pp 219−293.
(19) (a) Aime, S.; Botta, M.; Frullano, L.; Geninatti Crich, S.; Giovenzana, G. B.; Pagliarin, R.; Palmisano, G.; Sisti, M. *Chem.*−*Eur. J.* **1999**, *5*, 1253−1260. (b) Aime, S.; Benetollo, F.; Bombieri, G.; Colla, S.; Fasano, M.; Paoletti, S. *Inorg. Chim. Acta* **1997**, *254*, 63−70. (c) Ibrahim, M. A.; Haughton, V. M.; Hyde, J. S. *Am. J. Neuroradiol.* **1994**, *15*, 1907−1910. (d) Mukkala, V.-M.; Kwiatkowski, M.; Kankare, J.; Takalo, H. *Helv. Chim. Acta* **1993**, *76*, 893−899.
(20) Couchet, J. M.; Galaup, C.; Tisnès, P.; Picard, C. *Tetrahedron Lett.* **2003**, *44*, 4869−4872.
(21) Atkins, T. J.; Richman, J. E.; Oettle, W. F. *Org. Synth*. **1978**, *58*, 86−98.
(22) Newkome, G. R.; Pappalardo, S.; Gupta, V. K.; Fronczek, F. R. *J. Org. Chem.* **1983**, *48*, 4848−4851.

8.33 (d, 2H, ^3J = 7.5 Hz). ^{13}C NMR (D_2O, 50 MHz): δ 54.1, 54.7, 55.1, 57.3, 60.4, 125.4, 128.9, 146.3, 148.9, 154.5, 173.0, 174.5. MS (FAB$^+$, glycerol): *m/z* 458 ([M + H]$^+$, 100%). HRMS (FAB$^+$) Calcd for [M + H]$^+$ ($C_{22}H_{28}O_6N_5$): 458.20396. Found: 458.20415.

In Situ Preparation of L^3·Ln Complexes. An equimolar amount of $LnCl_3 \cdot nH_2O$ in water (2×10^{-3} M) was added to a solution of $\mathbf{L^3H_3}$ in water (2×10^{-3} M). The reaction mixture was stirred for 1 h at room temperature, and then it was adjusted to a final concentration of 1×10^{-5} M$-$$1 \times 10^{-6}$ M in HEPES buffer (0.05 M, pH 7.3). **L^3·La**. UV$-$vis: λ (ϵ) 250 (5950), 310 (11175), 321sh (9825). **L^3·Sm**. UV$-$vis: λ (ϵ) 249 (6925), 310 (12300), 321sh (11450). Luminescence (corrected spectrum, λ_{exc} = 310 nm): λ_{em} (relative intensity) 566 (20.5), 602 (100), 648 (66.6), 707 (54). **L^3·Eu**. UV$-$vis: λ (ϵ) 249 (6375), 310 (10625), 321sh (9325). Luminescence (corrected spectrum, λ_{exc} = 310 nm): λ_{em} (relative intensity) 582 (5.4), 595 (38.9), 617 (94.8), 652 (7.1), 695 (100). **L^3·Gd**. UV$-$vis: λ (ϵ) 250 (5575), 310 (10000), 322sh (9100). **L^3·Tb**. UV$-$vis: λ (ϵ) 249 (6000), 310 (10375), 321sh (9300). Luminescence (corrected spectrum, λ_{exc} = 310 nm): λ_{em} (relative intensity) 489 (53.5), 548 (100), 584 (46.5), 623 (46.5). **L^3·Dy**. UV$-$vis: λ (ϵ) 249 (6575), 310 (11475), 319sh (10500). Luminescence (corrected spectrum, λ_{exc} = 310 nm): λ_{em} (relative intensity) 484 (74.1), 578 (100). **L^3·Lu**. UV$-$vis: λ (ϵ) 250 (6675), 310 (11175), 319sh (11000).

Preparation of L^3·Eu. $EuCl_3 \cdot 6H_2O$ (18 mg, 0.049 mmol), dissolved in 1 mL of water, was added to a solution of $\mathbf{L^3H_3}$ (20 mg, 0.044 mmol) in a mixture of water (5 mL) and ethanol (3 mL). The resulting solution was stirred for 1 h, after which the pH was increased to 10 using Et_3N. The solvents were evaporated under reduced pressure, and the solid residue was redissolved in water. THF was added resulting in the formation of a precipitate, which was isolated by centrifugation, washed with THF, and dried under reduced pressure, yielding a yellow solid. Yield: 21 mg (72%). FT-IR (KBr): ν_{max} 1601 (C═O). MS (ESI$^+$, H_2O): *m/z* 646.2 ([M + K]$^+$, 14%), 630.1 ([M + Na]$^+$, 26%), 608.1 ([M + H]$^+$, 100%), Anal. Calcd for $C_{22}H_{24}N_5O_6Eu \cdot 3H_2O$: C, 40.01; H, 4.58; N, 10.60. Found: C, 39.74; H, 4.42; N, 10.36.

Preparation of L^3·Gd. $GdCl_3 \cdot 6H_2O$ (22.8 mg, 0.061 mmol) in 2 mL of water was added to a solution of $\mathbf{L^3H_3}$ (28.1 mg, 0.061 mmol) in water (5 mL), and the mixture was stirred for 1 h at room temperature. Then, the pH of the solution was brought to 8.0 using a 1 N NaOH solution in water. The mixture was evaporated to dryness, and the residue was solubilized in a minimum amount of methanol. Diethyl ether was added resulting in the formation of a white solid which was isolated after centrifugation. The complex was then dialyzed (cutoff of the membrane 500, Spectra-Por, VWR, Leuven, Belgium). The absence of free gadolinium ions was verified using the Arzenazo test. MS (ESI$^+$, H_2O): *m/z* 651.3 ([M + K]$^+$, 5%), 635.2 ([M + Na]$^+$, 100%).

Fluorescence, Phosphorescence, and Luminescence Measurements. Fluorescence spectra were obtained with a LS-50B Perkin-Elmer spectrofluorimeter equipped with a Hamamatsu R928 photomultiplier tube and operated using FLDM software. The energies of the 0$-$0 transition of the singlet states were determined by the intercept of the absorption and fluorescence spectra. The phosphorescence (**L^3H_3**, **L^3·La**, **L^3·Gd**, and **L^3·Lu** species) and luminescence (**L^3·Sm**, **L^3·Eu**, **L^3·Tb**, and **L^3·Dy** species) emission and excitation spectra were acquired using the same instrument operating in time-resolved mode. The excitation spectra were automatically corrected, and the emission spectra were corrected from the wavelength dependence of the photomultiplier tube, according to the instrument guidebook. Lifetimes, τ (uncertainty $\leq$ 5%), are the average values from at least 10 separate measurements covering two or more lifetimes. Liquid N_2 cooling was used to obtain the luminescence and phosphorescence spectra at low temperature (77 K). The phosphorescence spectra of the **L^3H_3**, **L^3·La**, **L^3·Gd**, and **L^3·Lu** species were recorded in a HEPES buffer/glycerol mixture (1/1). The triplet-state energy levels were determined from the shortest-wavelength phosphorescence bands, which were assumed to be the 0$-$0 transitions. The number of coordinated water molecules (q) were calculated from the following equations in which τ_H and τ_D are the lifetimes (in ms) of the complex in H_2O and D_2O, respectively: Parker's equation[23][q(Eu) = $1.2(1/\tau_H - 1/\tau_D - 0.25)$, q(Tb) = $5(1/\tau_H - 1/\tau_D - 0.06)$], Horrocks's equation[24] [q(Eu) = $1.11(1/\tau_H - 1/\tau_D - 0.31)$], Choppin's equation[25][q(Eu) = $1.05(1/\tau_H) - 0.70$], and Kimura's equation[26][q(Sm) = $0.0254(1/\tau_H) - 0.37$]. The luminescence quantum yields (uncertainty of $\pm$10%) were determined by the method described by Haas and Stein,[27] using $[Ru(bpy)_3]^{2+}$ in aerated water (Φ = 0.028)[28] for the Eu(III) complex or quinine sulfate in 1 N sulfuric acid (Φ = 0.546)[29] for the Tb(III) complex as standards. The **L^3·Eu** and **L^3·Tb** complexes were taken as references for the determination of the quantum yields of the **L^3·Sm** and **L^3·Dy** complexes, respectively.

NMR Measurements. Variable-temperature ^{17}O NMR measurements were recorded at 7.05 T on a Bruker AMX-300 spectrometer (Bruker, Karlsrhue, Germany). The temperature was controlled by a BVT-2000 unit. ^{17}O NMR measurements at natural abundance were performed on 2 mL samples contained in 10 mm o.d. tubes. The concentration of the **L^3·Gd** solution was equal to 8.47 mM. ^{17}O diamagnetic transverse-relaxation times of water were measured using the CPMG sequence (90° and 180° pulse lengths were 25 and 50 μs, respectively). All ^{17}O NMR spectra were proton decoupled. ^{17}O transverse-relaxation times of water in solutions containing the Gd complex were calculated from the spectral line width. Measurements of the longitudinal relaxation rates at 0.47 T were performed on a Minispec PC-20 (Bruker, Karlsrhue, Germany) at temperatures ranging from 5 to 45 °C and on a fast field cycling relaxometer Stelar (Mede, Italy) at 55, 65, and 75 °C. Transmetalation by zinc ions was evaluated by the decrease of the water longitudinal relaxation rate at 310 K and 20 MHz (Bruker Minispec PC-20) of buffered phosphate solutions (pH 7, [KH_2PO_4] = 0.026 mol/L, [Na_2HPO_4] = 0.041 mol/L) containing 2.5 mM gadolinium complex and 2.5 mM Zn.[30] The NMRD curves were obtained on a fast field cycling relaxometer Stelar (PV, Mede, Italy). Additional relaxation rates at 0.47, 1.4, and 7.05 T were obtained on a Minispec PC-20, mq-60, and Bruker AMX-300 spectrometer, respectively (Bruker, Karlsruhe, Germany). Fitting of the ^{1}H NMRD was performed with data-processing software using different theoretical models describing the nuclear-relaxation phenomena observed (Minuit, CERN Library).[31,32] The final concentration of the gadolinium complex solution was determined by proton relaxometry at 0.47 T.

(23) Beeby, A.; Clarkson, I. M.; Dickins, R. S.; Faulkner, S.; Parker, D.; Royle, L.; de Sousa, A. S.; Williams, J. A. G.; Woods, M. *J. Chem. Soc., Perkin Trans. 2* **1999**, 493$-$503.
(24) Supkowski, R. M.; Horrocks Jr., W. D. W. *Inorg. Chim. Acta* **2002**, *340*, 44$-$48.
(25) Barthelemy, P. P.; Choppin, G. R. *Inorg. Chem.* **1989**, *28*, 3354$-$3357.
(26) Kimura, T.; Kato, Y. *J. Alloys Compd.* **1998**, *275*$-$*277*, 806$-$810.
(27) Haas, Y.; Stein, G. *J. Phys. Chem.* **1971**, *75*, 3668$-$3677.
(28) Nakamaru, K. *Bull. Chem. Soc. Jpn.* **1982**, *55*, 2697$-$2705.
(29) Meech, S. R.; Phillips, D. *J. Photochem.* **1983**, *23*, 193$-$217.
(30) Laurent, S.; Vander Elst, L.; Copoix, F.; Muller, R. N. *Invest. Radiol.* **2001**, *36*, 115$-$122.

Scheme 1. Synthesis of L^3H_3[a]

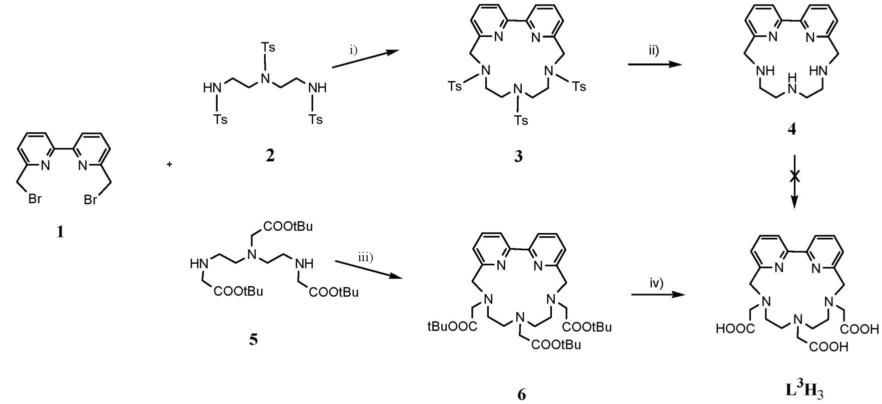

[a] (i) K_2CO_3, CH_3CN, reflux, [reactants] = 2.0×10^{-3} M; (ii) H_2SO_4, reflux; (iii) Na_2CO_3, CH_3CN, reflux, [reactants] = 2.4×10^{-3} M; (iv) CF_3COOH, CH_2Cl_2.

Results and Discussion

Synthesis of L^3H_3. As shown in numerous reports,[33] the macrocyclization process is the crucial step in the preparation of polyazamacrocyclic edifices. The synthesis of the bpyCTA-[15] ligand has been considered through two alternative approaches (Scheme 1): (i) by the classical Richman-Atkins method[34] and ii) by a macrocyclization reaction between 6,6′-bis(bromomethyl)-2,2′-bipyridine **1** and a 1,4,7-triazaheptane derivative **5** bearing three *tert*-butyl acetate groups. The presence of coordinating atoms in this triamine building block may control the formation of the 15-membered ring by a “metal-template” ion effect as shown in the preparation of the analogous 18-membered polyazamacrocycle derived from 2,2′:6′,2′′-terpyridine.[17]

Thus, the first synthetic approach involved the treatment of 1,4,7-tritosyl-1,4,7-triazaheptane **2** with the dibromo bipyridine fragment **1** by employing potassium carbonate as a base and acetonitrile as a solvent in heterogeneous conditions. This modified Richman−Atkins method[15,35] gives the macrocycle **3** in a better yield than that obtained by employing the classical procedure (77 vs 30%).[22] The tritosylated compound **3** was deprotected in concentrated sulfuric acid by heating (110 °C), according to the previously reported procedure,[22] giving ligand **4** in a 75% yield. Attempted alkylations were carried out by the reaction of **4** with chloroacetic acid at high pH (pH 10/KOH) in aqueous media at 80 °C or with *tert*-butyl bromoacetate in acetonitrile and in the presence of potassium carbonate as a base. Although these alkylating methods have been reported as successful in other polyazamacrocyclic systems,[36] they did not provide appreciable results in our hands.

In the second synthetic approach, the masked triacetate arms are incorporated prior to cyclization. The key building block **5**, 1,4,7-triazaheptane-1,4,7-triacetic acid tri-*tert*butyl ester, was prepared from commercially available diethylenetriamine following our previously reported procedure (overall yield: 74%).[11a] Treatment of **5** with 6,6′-bis(bromomethyl)-2,2′-bipyridine **1** was carried out in acetonitrile (reflux, 12 h) and in the presence of sodium carbonate as a base and without using high-dilution techniques (reactant concentration 2×10^{-3} M). The formation of the macrocycle-sodium complex (**6·Na**) as the only monomeric species was evidenced by ^{1}H NMR analysis of the crude mixture but some dissociation of **6·Na** occurred when purification was achieved by chromatography on alumina, and as a result, **6·Na** and the free ligand **6** were isolated in 12 and 22% yields, respectively. The ^{1}H NMR spectra of these two species display significant differences, reflecting the rigidity of the macrocyclic system because of the presence of the sodium ion. Full deprotection of *tert*-butyl esters in **6·Na** or **6** to reach the target L^3H_3 (80−85%) was cleanly achieved with a TFA−CH_2Cl_2 mixture (room temperature, 24 h).

Photophysical Properties. Complexation reactions were carried out in aqueous solution, typically by the addition of equimolar quantities of the appropriate lanthanide chloride to the aqueous solution of ligand L^3H_3 at pH 7.3. The complexation was detected by a red shift in the ligand absorption spectrum upon the addition of the lanthanide salt (vide infra). The equilibria were reached after 10 h at room temperature. In the case of the L^3·Eu complex, we noticed that the emitting properties in aqueous solution of the isolated complex (see Experimental Section) are identical to those

(31) Muller, R. N.; Declercq, D.; Vallet, P.; Giberto, F.; Daminet, B.; Fischer, H. W.; Maton, F.; Van Haverbeke, Y. In *Proceedings of the ESMRMB, 7th Annual Congress*, Strasbourg, France, 1990; European Society for Magnetic Resonance in Medicine and Biology: Vienna, Austria, 1990; p 394.

(32) Vallet, P. Relaxivity of Nitroxide Stable Free Radicals. Evaluations by Field Cycling Method and Optimisation. Ph.D. Thesis, University of Mons-Hainaut, Belgium, 1992.

(33) Bradshaw, J. S.; Krakowiak, K. E.; Izatt, R. M. In *Aza-Crown Macrocycles*; Wiley: New York, 1993.

(34) Richman, J. E.; Atkins, T. J. *J. Am. Chem. Soc.* **1974**, *96*, 2268−2270.

(35) Bazzicalupi, C.; Bencini, A.; Fusi, V.; Giorgi, C.; Paoletti, P.; Valtancoli, B. *J. Chem. Soc., Dalton Trans.* **1999**, 393−399.

(36) (a) Aime, S.; Gianolio, E.; Corpillo, D.; Cavallotti, C.; Palmisano, G.; Sisti, M.; Giovenzana, G. B.; Pagliarin, R. *Helv. Chim. Acta* **2003**, *86*, 615−632. (b) Siaugue, J.-M.; Segat-Dioury, F.; Sylvestre, I.; Favre-Reguillon, A.; Foos, J.; Madic, C.; Guy, A. *Tetrahedron* **2001**, *57*, 4713−4718. (c) Aime, S.; Botta, M.; Frullano, L.; Geninatti Crich, S.; Giovenzana, G.; Pagliarin, R.; Palmisano, G.; Riccardi Sirtori, F.; Sisti, M. *J. Med. Chem.* **2000**, *43*, 4017−4024. (d) Siaugue, J.-M.; Segat-Dioury, F.; Favre-Reguillon, A.; Madic, C.; Foos, J.; Guy, A. *Tetrahedron Lett.* **2000**, *41*, 7443−7446. (e) Horiguchi, D.; Katayama, Y.; Sasamoto, K.; Terasawa, H.; Sato, N.; Mochizuki, H.; Ohkura, Y. *Chem. Pharm. Bull.* **1992**, *40*, 3334−3337.

Table 1. Ligand-Centered Absorption and Emission Maxima

	$\pi \rightarrow \pi^{*a}$ λ_{max} (nm) (log ϵ)	$^1\pi\pi^{*a,b}$ λ_{max} (nm)	$^3\pi\pi^{*c,d}$ λ_{max} (nm)	τ ($^3\pi\pi^*$)^e (ms)
L^3H_3	301 (4.00)	335 (31450)	471 (22600)	750
L^3·La	310 (4.05)	345 (30550)	476 (22300)	160
L^3·Sm	310 (4.09)	*f*	*f*	*f*
L^3·Eu	310 (4.03)	*f*	*f*	*f*
L^3·Gd	310 (4.00)	343 (30600)	475 (22400)	3.1
L^3·Tb	310 (4.02)	*f*	*f*	*f*
L^3·Dy	310 (4.06)	*f*	*f*	*f*
L^3·Lu	310 (4.05)	343 (30600)	479 (22200)	106

[a] In HEPES buffer (pH 7.3) solutions at 295 K. [b] From fluorescence spectra, λ are given for the maximum of the band envelope, and the energies of the 0−0 transition (within parentheses) are given in cm^{-1}. [c] From phosphorescence spectra at 77 K, in HEPES buffer (pH 7.3)/glycerol (1/1). [d] The energies of the 0−0 transition (within parentheses) are given in cm^{-1}. [e] Lifetimes of the ligand $^3\pi\pi^*$ states at 77K. [f] $^1\pi\pi^*$ fluorescence and $^3\pi\pi^*$ phosphorescence quenched by transfer to the Ln ion.

of the complex formed in situ from equimolar mixtures of ligand and $EuCl_3$. Titration experiments recording the changes in the europium luminescence intensity upon ligand excitation and ESI mass spectrometry analyses (Figure S3, Supporting Information) allowed a 1:1 ligand−metal stoichiometry to be established in solution. This 1:1 stoichiometry is in good agreement with that obtained in the solid state by elemental analysis. We thus emphasized the in situ method and collected the photophysical data from the absorption, fluorescence, and luminescence spectra of **L^3·Ln** complexes measured after 15 h in HEPES buffer (50 mM, pH 7.3).

Ligand-Centered Transitions. Relevant photophysical data for the free ligand and La, Sm, Eu, Gd, Tb, Dy, and Lu complexes are presented in Table 1. The electronic spectrum of the free ligand **L^3H_3** in aqueous solution displays two absorption bands with maxima at 247 and 301 (shoulder 313) nm. These two bands attributed to $\pi \rightarrow \pi^*$ transitions centered on the 2,2′-bipyridine group are shifted by 15 and 22 nm toward longer wavelengths compared to those of the free 2,2′-bipyridine (232 and 279 nm), which exists in a trans conformation.[37] Similar red shifts were observed for the monoprotonated 2,2′-bipyridine which has a cis conformation, stabilized by a cationic hydrogen bond.[37a,38] This suggests the presence of a bipyridine subunit in a cis conformation in the macrocyclic structure of **L^3H_3**. Complexation with lanthanide chlorides resulted in a bathochromic shift of the maxima ($\Delta\nu$ = 9 nm for the low-energy absorption band). These are the expected shifts for a pertubation produced by the coordinated lanthanide ion which have been observed in other Ln(III) complexes with ligands derived from 2,2′-bipyridine.[39] At room temperature, irradiation of the free ligand through its $\pi \rightarrow \pi^*$ transitions results in a weak fluorescence from the $^1\pi\pi^*$ state characterized by a broad band centered at 335 nm. This assignment is corroborated by the complete disappearance of this band in the time-resolved emission spectrum (delay time 0.1 ms). In a rigid matrix at 77 K, this short-lived fluorescence is accompanied by a second band extending from 420 to 600 nm. It is structured, with a maximum at 471 nm and a single-exponential time decay with a lifetime of 750 ms. It is therefore a phosphorescence band originating from the $^3\pi\pi^*$ state. From the highest-energy phosphorescence feature of **L^3H_3**, the position of the lowest ligand-centered $^3\pi\pi^*$ excited state is estimated to be about 22600 cm^{-1}.

The lowest-lying MC excited level of the Gd^{3+} ion ($^6P_{7/2}$, E = 32150 cm^{-1})[40] is higher than the singlet and triplet state of **L^3H_3** (Figure S4, Supporting Information), and the energy cannot be transferred to the gadolinium from the chromophoric moiety of this ligand. So, the **L^3·Gd** complex displays essentially the same fluorescence and phosphorescence features as the free ligand. In **L^3·Gd**, the energies of the lowest ligand-centered excited states ($^1\pi\pi^*$ and $^3\pi\pi^*$ states) are moderately shifted (850 and 200 cm^{-1}, respectively). The effect from the metal ion is more apparent on the rate of deactivation of the triplet excited state, whose lifetime at 77 K is decreased by about 2.4 orders of magnitude compared to that of the free ligand. It seems likely that this decrease in lifetime is the result of an increase of the rate of the $^1\pi\pi^* \rightarrow {}^3\pi\pi^*$ intersystem crossing, caused by the presence of the paramagnetic metal ion. Similar trends were observed for **L^3·La** and **L^3·Lu** complexes (i.e., the magnitude of the red shift of the lowest ligand-centered excited states and the shorter phosphorescence lifetime). In contrast, in the **L^3·Ln** (Ln = Sm, Eu, Tb, Dy) complexes, the emissions from the ligand-centered states are completely quenched and the characteristic emission bands of these lanthanide ions appear in the spectrum, pointing out a complete ligand-to-metal energy transfer (Figure 1).

Eu- and Tb-Centered Luminescence. Upon excitation into either of the aforementioned absorbance bands, the **L^3·Eu** and **L^3·Tb** complexes also exhibit, at room temperature and in aqueous solution, bright red and green luminescence, respectively. In these complexes, the strongest emissions are located around 615 and 545 nm, which correspond to the Eu^{3+}-centered $^5D_0 \rightarrow {}^7F_2$ and Tb^{3+}-centered $^5D_4 \rightarrow {}^7F_5$ hypersensitive transitions, respectively. The similarity between the absorption and excitation spectra confirms that the population of the Eu^{3+} and Tb^{3+} excited states takes place through the bipyridine antenna. The temporal decay of the emission of both complexes was rigorously monoexponential showing that both Eu^{3+} and Tb^{3+} ions lie in the same average chemical environment in aqueous solution; lifetimes are in the millisecond range and are given in Table 2. The efficiency of the overall sensitization process was established by determining the quantum yields (Φ) of emission, following excitation into the organic chromophore, which are 0.10 for **L^3·Eu** and 0.21 for **L^3·Tb**. These Φ values are among the largest reported in aqueous solutions for either Eu^{3+} or Tb^{3+}

(37) (a) Nakamoto, K. *J. Phys. Chem.* **1960**, *64*, 1420−1425. (b) Howard, S. T. *J. Am. Chem. Soc.* **1996**, *118*, 10269−10274.
(38) (a) Krumholz, P. *J. Am. Chem. Soc.* **1951**, *73*, 3487−3492. (b) Westheimer, F. H.; Benfey, O. T. *J. Am. Chem. Soc.* **1956**, *78*, 5309−5311. (c) Linnell, R. H.; Kaczmarczyk, A. *J. Phys. Chem.* **1961**, *65*, 1196−1200.
(39) Sabbatini, N.; Guardigli, M.; Lehn, J.-M. *Coord. Chem. Rev.* **1993**, *123*, 201−228.
(40) Stein, G.; Würzberg, E. *J. Chem. Phys.* **1975**, *62*, 208−213.

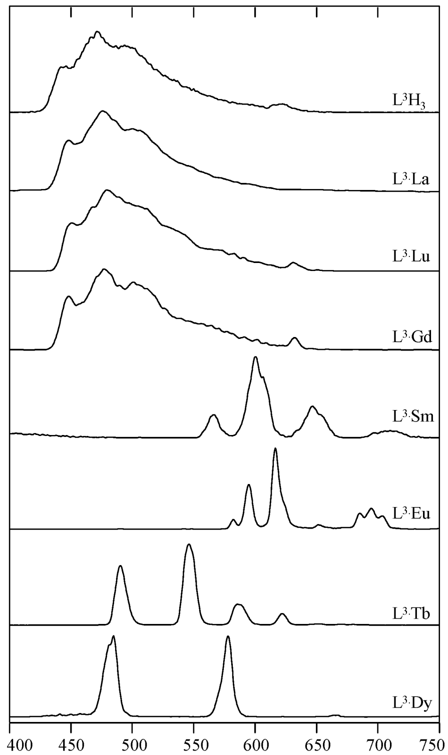

Figure 1. Noncorrected phosphorescence emission spectra measured at 77 K in HEPES buffer (pH 7.3) for $\mathbf{L^3H_3}$ and $\mathbf{L^3{\cdot}Ln}$ complexes (Ln = Sm, Eu, Tb, Dy) and in HEPES buffer (pH 7.3)/glycerol (1/1) for $\mathbf{L^3{\cdot}Ln}$ complexes (Ln = La, Lu, Gd): λ_{ex} = 301 nm ($\mathbf{L^3H_3}$) and 310 nm ($\mathbf{L^3{\cdot}Ln}$), excitation and emission passes = 5 nm.

complexes containing one or more 2,2′-bipyridine chromophores.[11c,11d,39,41−43] On the other hand, with respect to pyridine-containing $\mathbf{L^1{\cdot}Ln}$ complexes, $\mathbf{L^3{\cdot}Eu}$ and $\mathbf{L^3{\cdot}Tb}$ are three and two times more luminescent, respectively. Information about the hydration number, *q* (which provides the number of metal-bound water molecules), may be gained by comparison of the lifetimes of Eu^{3+} and Tb^{3+} complexes in protonated and deuterated water and by use of the empirical relationship developed by Parker and co-workers.[23] This relationship takes into account the effect of outer-sphere water molecules and shows that 1.19 and 1.18 water molecules are coordinated to Eu^{3+} and Tb^{3+} ions, respectively, complexed by $\mathbf{L^3}$. The use of a refined equation, recently proposed on the basis of europium complexes and validated in a larger range of *q* values,[24] yields $q = 1.04$ for $\mathbf{L^3{\cdot}Eu}$. These results clearly indicate that there is only one metal-bound water molecule in each complexes. The coordination number of the aqueous Eu^{3+} and Tb^{3+} ions is 9 (Ln·$[H_2O]_9$ species),[44] which strongly suggests that the eight binding sites provided by the ligand $\mathbf{L^3H_3}$ are coordinated to the lanthanide ion.

The sensitization pathway, which seems to be general in Eu^{3+} and Tb^{3+} complexes, proceeds through intersystem crossing (ISC) from the excited singlet state to the triplet state of the antenna, followed by an intramolecular energy transfer from the triplet state to the closest emitting level of the metal. On the other hand, for ligand-sensitized europium and terbium luminescence, factors limiting radiative decay processes are well documented.[39,42,45] Besides the luminescence quenching by bound and closely diffusing water molecules, a back-energy transfer process between the metal ^5D_j and ligand $^3\pi\pi^*$ excited states and the involvement of ligand to Eu^{3+} charge-transfer excited states (LMCT states) may constitute significant terms in the overall quenching effect. No large increase in the lifetime of the terbium-centered emission is observed when the temperature is lowered to 77 K. This relatively weak temperature dependence of the lifetime is reflected in the low value (160 s^{-1}) of the nonradiative temperature-dependent decay rate constant $k_{nr}(T)$, obtained by taking the difference of the reciprocal lifetimes in D_2O at 298 and 77 K. As a comparison, Sabbatini et al.[39] reported a value of 1300 s^{-1} for $k_{nr}(T)$ for a Tb^{3+} cryptate, in which an equilibrium between the chromophoric donor and Tb acceptor occurs at room temperature. This indicates that thermally activated back-energy transfer ($^5D_4 \rightarrow {}^3\pi\pi^*$), which is observed particularly for the Tb^{3+} complexes of the bipyridine-based ligands,[11c,11d,39,41] is rather inefficient in $\mathbf{L^3{\cdot}Tb}$. This result is consistent with the work of Latva et al., who suggested that a fast and irreversible energy transfer to Tb^{3+} ion occurs when an energy gap, ΔE ($E[^3\pi\pi^*] - E[^5D_4]$), is greater than 1850 cm^{-1}.[42] In $\mathbf{L^3{\cdot}Tb}$, this energy gap, measured as usual from the ligand phosphorescence spectrum of $\mathbf{L^3{\cdot}Gd}$ ($E_{00}[^3\pi\pi^*] = 22\,400$ cm^{-1}), is estimated to be 1900 cm^{-1} and, consequently, is slightly above this threshold value. As far as the $\mathbf{L^3{\cdot}Eu}$ complex is concerned and looking at this energy value of 22 400 cm^{-1}, energy transfer to Eu^{3+} is feasible to its $^5D_0$, $^5D_1$, and $^5D_2$ levels (ΔE = 5100, 3400, and 900 cm^{-1}, respectively). In this complex**,** back transfer to the ligand triplet state does not seem to play a role since the rate constant is temperature independent. This suggests that the energy is transferred either directly to the emitting $^5D_0$ level or to the $^5D_1$ state level which decays nonradiatively to the lower-lying $^5D_0$ level. The lack of equilibration between the triplet excited state and the emitting level of the metal is also supported by the lack of luminescence quenching by dioxygen. No substantial increase of intensities and lifetimes is observed

(41) (a) Vila-Nova, S. P.; Pereira, G. A. L.; Albuquerque, R. Q.; Mathis, G.; Bazin, H.; Autiero, H.; de Sa, G. F.; Alves, S., Jr. *J. Lumin.* **2004**, *109*, 173−179. (b) Weibel, N.; Charbonnière, L. J.; Guardigli, M.; Roda, A.; Ziessel, R. *J. Am. Chem. Soc.* **2004**, *126*, 4888−4896. (c) Couchet, J.-M.; Azéma, J.; Tisnès, P.; Picard, C. *Inorg. Chem. Commun.* **2003**, *6*, 978−981. (d) Bodar-Houillon, F.; Heck, R.; Bohnenkamp, W.; Marsura, A. *J. Lumin.* **2002**, *99*, 335−341. (e) Ulrich, G.; Bedel, S.; Picard, C. *Tetrahedron Lett.* **2002**, *43*, 8835−8837. (f) Charbonnière, L.; Ziessel, R.; Guardigli, M.; Roda, A.; Sabbatini, N.; Cesario, M. *J. Am. Chem. Soc.* **2001**, *123*, 2436−2437. (g) Ulrich, G.; Ziessel, R.; Manet, I.; Guardigli, M.; Sabbatini, N.; Fraternali, F.; Wipff, G. *Chem.*−*Eur. J.* **1997**, *3*, 1815−1822. (h) Sabbatini, N.; Guardigli, M.; Manet, I.; Ungaro, R.; Casnati, A.; Ziessel, R.; Ulrich, G.; Asfari, Z.; Lehn, J.-M. *Pure Appl. Chem.* **1995**, *67*, 135−140.

(42) Latva, M.; Takalo, H.; Mukkala, V.-M.; Matachescu, C.; Rodriguez-Ubis, J.-C.; Kankare, J. *J. Lumin.* **1997**, *75*, 149−169.

(43) (a) Alpha, B.; Ballardini, R.; Balzani, V.; Lehn, J.-M.; Perathoner, S.; Sabbatini, N. *Photochem. Photobiol.* **1990**, *52*, 299−306. (b) Bazin, H.; Preaudat, M.; Trinquet, E.; Mathis, G. *Spectrochim. Acta A* **2001**, *57*, 2197−2211.

(44) Horrocks, W. D. W., Jr.; Sudnick, D. R. *J. Am. Chem. Soc.* **1979**, *101*, 334−340.

(45) Parker, D.; Williams, J. A. G. *J. Chem. Soc., Dalton Trans.* **1996**, 3613−3628.

Table 2. Metal Luminescent Data of $\mathbf{L^3{\cdot}Ln}$ Complexes (Ln = Eu, Tb, Sm, Dy)[a]

	$\tau(H_2O)$ (ms)	$\tau(D_2O)$ (ms)	q[b]	$k_{nr}(OH)$[c] (s^{-1})	$k_{nr}(T)$[d] (s^{-1})	$\Phi(H_2O)$ ($\times 10^2$)	$\Phi(D_2O)$ ($\times 10^2$)	ΔE[e] (cm^{-1})
$\mathbf{L^3{\cdot}Eu}$	0.56 (0.87)[f]	1.84 (1.85)[f]	1.19	1250	0	10	26	5100
$\mathbf{L^3{\cdot}Tb}$	1.28 (1.82)[f]	2.06 (2.54)[f]	1.18	300	160	21	27	1900
$\mathbf{L^3{\cdot}Sm}$	0.015	0.034 (0.034)[f]	1.32	37250	0	0.06		4500
$\mathbf{L^3{\cdot}Dy}$	< 0.010	(0.035)[f]				0.06		1300

[a] Data obtained in aerated HEPES buffer (pH 7.3) at 298 K. [b] Number of coordinated H_2O molecules estimated with the Parker equation.[23] [c] From the lifetimes in H_2O and D_2O solutions at 298 K, $k_{nr}(OH) = 1/\tau_H^{298K} - 1/\tau_D^{298K}$. [d] From the lifetimes in D_2O solution at 298 and 77 K, $k_{nr}(T) = 1/\tau_D^{298K} - 1/\tau_D^{77K}$. [e] Energy difference between the 0-phonon triplet ligand level measured in $\mathbf{L^3{\cdot}Gd}$ (22 400 cm^{-1}) and the Ln first excited state; $E(Eu-{}^5D_0) = 17\,300$ cm^{-1}, $E(Tb-{}^5D_4) = 20\,500$ cm^{-1}, $E(Sm-{}^4G_{5/2}) = 17\,900$ cm^{-1}, $E(Dy-{}^4F_{9/2}) = 21\,100$ cm^{-1}. [f] Data obtained at 77 K.

upon degassing of the solutions, suggesting that the triplet state of the chromophoric bipyridine is not subject to deactivation by dissolved molecular oxygen. On the other hand, in $\mathbf{L^3{\cdot}Eu}$, a quenching mechanism through a low-lying charge transfer state may occur because of the low reduction potential of the Eu^{3+} ion[46] and the presence of the electron pairs of the aliphatic nitrogens. Direct observation of LMCT transitions in the absorption spectra of $\mathbf{L^3{\cdot}Eu}$ is not possible because of their much smaller extinction coefficients compared with those of the ligand centered bands. In some cases, it was established[47] that coordination of the F^- anion to the Eu^{3+} ion shifts the LMCT bands of the complex to higher energies, thus limiting radiationless decay via low-lying charge-transfer levels. Our experiments with fluoride ions indicate that this anion displaces water from the solvation sphere (vide infra), but no additional effect was seen. Moreover, the temperature independence of the lifetime of this complex indicates that no upper-lying LMCT state is thermally accessible from the $^5D_0$ emitting state. These results suggest that the main quenching pathway for the Eu^{3+} and Tb^{3+} luminescence in $\mathbf{L^3{\cdot}Eu}$ and $\mathbf{L^3{\cdot}Tb}$ complexes is the product of the high-energy vibrational modes of one coordinated water molecule. This is supported by the similar Φ values of these two complexes in deuterated water.

Sm- and Dy-Centered Luminescence. Emission spectra of $\mathbf{L^3{\cdot}Sm}$ and $\mathbf{L^3{\cdot}Dy}$ show that the same photosensitization process discussed for $\mathbf{L^3{\cdot}Eu}$ and $\mathbf{L^3{\cdot}Tb}$ also occurs in these complexes. The excitation spectra registered at the maximum of the Sm^{3+} or Dy^{3+} emission match the absorption spectra of the complexes, both at 77 and 298 K (see Figure S5, Supporting Information). The luminescence lifetimes of these two complexes lie in the microsecond range, and their quantum yields are rather low ($<10^{-3}$) (see Table 2). Using Kimura's equation,[26] we calculated that one water molecule is essentially present in the first coordination sphere of the samarium ion, in line with previous observations for the europium and terbium complexes. The calculated rate constant $k_{nr}(OH)$ for $\mathbf{L^3{\cdot}Sm}$ is 37 250 s^{-1}; this value compared to the values of 600 s^{-1} for $\mathbf{L^3{\cdot}Eu}$ and 150 s^{-1} for $\mathbf{L^3{\cdot}Tb}$ emphasizes the greater sensitivity of Sm^{3+} toward quenching by O−H vibrations. The lifetime of $\mathbf{L^3{\cdot}Dy}$ cannot be measured accurately at room temperature because of the instrumental set up. As one can see from Table 2, short lifetime values were also obtained at 77 K in D_2O solution. Although the energy difference between the ligand-centered triplet state and the $^4F_{9/2}$ state of Dy^{3+} is only 1300 cm^{-1}, it is worth noting the absence of the $^3\pi\pi^*$ emission from $\mathbf{L^3{\cdot}Dy}$ at 77 K.

The features of the metal-centered emission (τ, Φ) observed for $\mathbf{L^3{\cdot}Sm}$ and $\mathbf{L^3{\cdot}Dy}$ are in the expected range. As a matter of fact, the lifetime and quantum yield reported for well-protected Sm^{3+} and Dy^{3+} organosystems rarely exceed respectively 100 μs and 2%, respectively, in aqueous medium.[6e,48] This weak luminescence is related to the small energy gap between the lowest luminescent state and the highest J level of the ground state of these ions ($\Delta E \approx 7000-8000$ cm^{-1} vs 12000−14000 cm^{-1} for Eu^{3+} and Tb^{3+}).[40]

Stability in Aqueous Media. The stability in solution of a Ln^{III} complex is of outstanding importance for the selection of a chelator as far as biological applications are concerned. There are many factors influencing the stability of a metal chelate in biological media including the competition of protons, endogenous cations (such as Ca^{2+} and Zn^{2+}) or anions (hydroxyde and phosphate) and native chelators (e.g., albumin and transferrin). Thus, the in vivo stability of a metal chelate is predominantly determined by its kinetic inertness rather than its thermodynamic stability.[49] In vitro studies reported recently the important role played by Zn^{2+} in the release of Gd^{3+} from the complex $[DTPA{\cdot}Gd]^{2-}$, the first chelate to enter clinical practice which is currently used in a number of pathologies. It has been established that the dissociation of $[DTPA{\cdot}Gd]^{2-}$ predominantly occurs through the direct attack of Zn^{2+} on the complex.[50] In this work, the stability studies (Figure S6, Supporting Information) were conducted by luminescence spectroscopy with the europium complex. As a matter of fact, a particularly useful feature of

(46) Morss, L. R. *Chem. Rev.* **1976**, *76*, 827−841.
(47) Sabbatini, N.; Perathoner, S.; Lattanzi, G.; Dellonte, S.; Balzani, V. *J. Phys. Chem.* **1987**, *91*, 6136−6139.
(48) (a) Gonçalves e Silva, F. R.; Malta, O. L.; Reinhard, C.; Güdel, H.-U.; Piguet, C.; Moser, J. E.; Bünzli, J.-C. G. *J. Phys. Chem. A* **2002**, *106*, 1670−1677. (b) Brunet, E.; Juanes, O.; Sedano, R.; Rodriguez-Ubis, J.-C. *Photochem. Photobiol. Sci.* **2002**, *1*, 613−618. (c) Hakala, H.; Liitti, P.; Puukka, K.; Peuralahti, J.; Loman, K.; Karvinen, J.; Ollikka, P.; Ylikoski, A.; Mukkala, V.-M.; Hovinen, J. *Inorg. Chem. Commun.* **2002**, *5*, 1059−1062. (d) Zucchi, G.; Ferrand, A.-C.; Scopelliti, R.; Bünzli, J.-C. G. *Inorg. Chem.* **2002**, *41*, 2459−2465. (e) Rodriguez-Ubis, J.-C.; Sedano, R.; Barroso, G.; Juanes, O.; Brunet, E. *Helv. Chim. Acta* **1997**, *80*, 86−96.
(49) (a) Liu, S.; Edwards, D. S. *Bioconjugate Chem.* **2001**, *12*, 7−34. (b) Crooks, W. J.; Choppin, G. R.; Rogers, B. E.; Welch, M. J. *Nucl. Med. Biol.* **1997**, *24*, 123−125. (c) Parker, D. In *Comprehensive Supramolecular Chemistry*, Vol 10; Lehn J.-M., Ed.; Pergamon: Oxford, 1996; p 487. (d) Amin, S.; Morrow, J. R.; Lake, C. H.; Churchill, M. R. *Angew. Chem., Int. Ed. Engl.* **1994**, *33*, 773−775.
(50) Sarka, L.; Burai, L.; Brücher, E. *Chem.−Eur. J.* **2000**, *6*, 719−724.

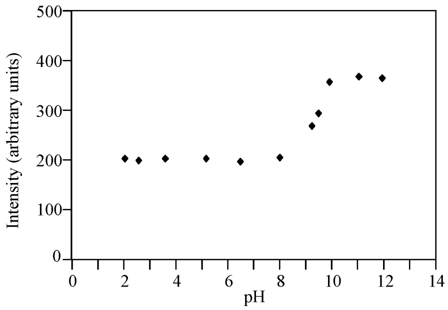

Figure 2. pH dependence of the total luminescence emission for **L^3·Eu**.

the Eu^{III} ion (vs Tb^{III} ion) is that its emission spectrum and lifetime have been found to be reliable indicators of the metal solution-phase coordinating chemistry.[5a,51]

L^3·Eu showed a remarkable kinetic stability in aqueous solution over a wide pH range, indicating the absence of any dissociation process in this interval. In the pH range between 2 and 8.5, the total emission intensity and emission lifetime ($\tau = 0.56$ ms) exhibited no variation with the pH of the solution. Spectra recorded at pHs of >10 were much more intense than those measured in more acidic media (Figure 2). The emission intensity was increased by a factor 1.8, and the emission lifetime reached a value of 0.80 ms. The use of Barthelemy and Choppin relationship[25] between the hydration number of the Eu^{III} ion and the luminescence decay constant obtained only in H_2O solution allows an estimation of the apparent hydration state (q) of the complex. This analysis gave q values of 1.2 (pH range 2−8) and 0.6 (pH range 10−12). The fact that there is a decrease in the number of O−H oscillators with increasing pH was correlated to the replacement of one water molecule (i.e., 2 O−H oscillators) with one hydroxyl ion (i.e., 1 O−H oscillator) in the inner coordination sphere (or the deprotonation of the coordinated water molecule). The environment change around Eu^{III} as a function of pH was also validated by the change in the value of the ratio $^5D_0 \rightarrow {}^7F_2/{}^5D_0 \rightarrow {}^7F_1$ emission intensity (2.1 and 2.9 at pH 6.5 and 11, respectively).

Although Ca^{2+} and Eu^{3+} ions present similar features, no Ca^{2+}-promoted dissociation was observed after several days when **L^3·Eu** (10 μM) was incubated at room temperature and physiological pH in the presence of an excess of calcium (126 mM). The luminescence intensity and lifetime of **L^3·Eu** also remained unchanged in the presence of other abundant human serum cations (Mg^{2+}, 0.8 mM; Zn^{2+}, 0.01mM; Na^+, 140 mM; K^+, 5mM), indicating the resistance of this europium complex to dissociation in the presence of these competing cations. The sensitivity of **L^3·Eu** to fluoride ions was also studied. It has been established that this small-hard charged anion can displace the residual H_2O molecule from the coordination sphere of Eu^{3+}, reducing the H_2O quenching.[47,52] A 2-fold increase of the total emission intensity and a lower value in the $^5D_0 \rightarrow {}^7F_2/{}^5D_0 \rightarrow {}^7F_1$ ratio were observed with a saturating anion concentration (400 mM, F^-). These changes in both the intensity and the profile of the emission spectrum (Figure 3) are consistent with the

(51) Choppin, G. R.; Peterman, D. R. *Coord. Chem. Rev.* **1998**, *174*, 283−299.

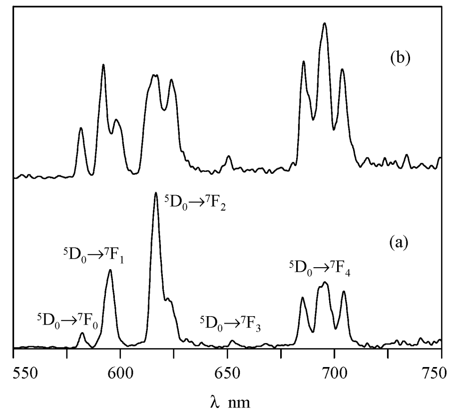

Figure 3. Corrected emission spectra of **L^3·Eu** (1.2×10^{-5} M in HEPES buffer) in the presence of fluoride ions: (a) no fluoride and (b) 0.4 M fluoride. $\lambda_{ex} = 310$ nm. excitation and emission passes = 2.5 nm.

involvement of fluoride ion in the coordination to the metal. The displacement of water from the coordination sphere of the metal was also reflected by the lengthening of the luminescence lifetime (1.08 ms vs 0.56 ms in the absence of F^-). The monoexponential decay curve observed suggests a rapid exchange process between coordinated water and fluoride ions on the time scale of the excited state. No displacement of the ligand by phosphate anions (5×10^3 fold excess) which would result in a decrease of luminescence intensity was seen in our experiments. On the contrary, the **L^3·Eu**−phosphate system exhibited effects analogous to those found for **L^3·Eu**−F^- (i.e., an enhancement in both the lifetime ($\tau = 0.85$ ms) and the emission signal and changes in the emission spectrum). These effects are less important than those observed with F^- ion, probably in relation to the bulkiness of the phosphate group compared to that of the fluoride anion. In vitro human serum stability of **L^3·Eu** was used as an additional indicator of in vivo stability. No dissociation was noticed up to 48 h when the complex (10 μM) was incubated in a mixture of HEPES buffer/human serum (2/1) at pH 7.3 (Figure 4). Furthermore, the lifetime (characterized by a monoexponential decay) and the shape of the emission spectrum remained unchanged, suggesting that no interaction occurs between the complex and serum proteins. The lack of binding between **L^3·Eu** and albumin was also observed by experiments setting bovine serum albumin in action.

We also studied the resistance of the **L^3·Eu** complex to dissociation in the presence of an another poly(aminocarboxylate) chelating ligand for which stability constants with lanthanide ions have been reported. The competing ligand chosen was DOTA which binds strongly to Eu^{3+} (K(Eu) = 5×10^{23})[53] and forms an Eu^{3+} complex that does not luminesce upon excitation at 310 nm at the concentration used (10 μM). In the presence of a 5-fold excess of DOTA at pH 7.3 (HEPES buffer), 30% of the **L^3·Eu** complex was dissociated, allowing one month for equilibration. Using the

(52) (a) Cross, J. P.; Dadabhoy, A.; Sammes, P. G. *J. Lumin.* **2004**, *110*, 113−124. (b) Coates, J.; Gay, E.; Sammes, P. G. *Dyes Pigm.* **1997**, *34*, 195−205.

(53) Cacheris, W. P.; Nickle, S. K.; Sherry, A. D. *Inorg. Chem.* **1987**, *26*, 958−960.

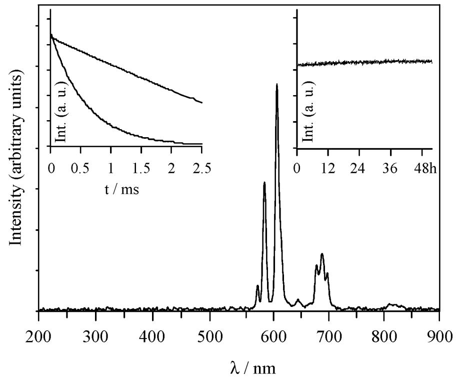

Figure 4. Noncorrected luminescence spectrum of **L^3·Eu** in HEPES buffer/human serum (2/1): $\lambda_{exc} = 310$ nm, delay time/gate time = 0.1/0.4 ms, excitation and emission passes = 5 nm. The left inset shows the excited-state lifetime, luminescence decay curve (bottom plot), and ln(intensity) versus time (upper plot). The right inset shows the luminescence intensity of the $^5D_0 \rightarrow {}^7F_2$ emission band as a function of time.

Verhoeven method,[54] this preliminary result suggests a conditional stability constant for **L^3·Eu** higher than 10^{18}.

Relaxivity Properties of the L^3·Gd Complex. Gadolinium complexes are known to increase the relaxation rates of water protons by short-distance magnetic interactions between the water protons and the lanthanide ion (inner-sphere contribution) and by longer-distance magnetic interactions (outer-sphere contribution). The inner-sphere contribution described by Solomon and Bloembergen[55,56] results from the presence of one (or more) water molecule(s) in the first coordination sphere of the ion and from its (their) exchange with bulk water. It is thus closely related to the distance between the proton of the coordinated water molecule and the ion (r), to the rotational mobility of the hydrated complex and thus to its size, and to the exchange rate of the water molecule. The outersphere mechanism as described by Freed[57] comes from the magnetic interaction between unbound water molecules diffusing in the close proximity of the ion. This mechanism depends on the distance of closest approach between the water molecules and the ion (d) and on the relative translational diffusion constant (D). For some complexes, an additional second-sphere contribution has been involved.[58] This contribution results from a second-sphere of hydration molecules exchanging with bulk water. It is described by a model similar to the inner-sphere one but the distance of interaction (r_{SS}) is larger and the exchange rate of the water molecules is much faster.

Residence Time of the Water Molecule Coordinated to the L^3·Gd Complex. It is now well established that the residence time of water molecules in the first coordination sphere of a gadolinium complex (τ_M) can be obtained from the analysis of the temperature dependence of the ^{17}O transverse-relaxation rate of water in the **L^3·Gd** solution. In

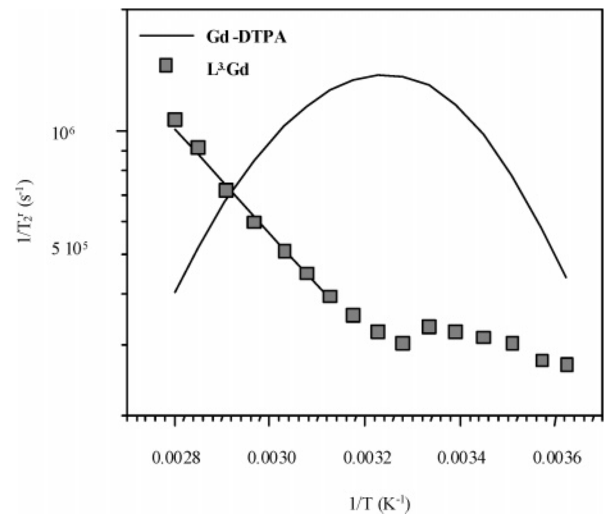

Figure 5. ^{17}O reduced transverse-relaxation rate ($1/T_2^r$) as a function of the reciprocal of the temperature for aqueous solutions of **L^3·Gd** and **Gd–DTPA**. The lines correspond to the theoretical fits to the data points.

the temperature range investigated (276 K to 357 K), the evolution of the reduced transverse-relaxation rate of ^{17}O ($1/T_2^r = 55.55/(T_2q[\mathbf{L^3{\cdot}Gd}])$) differs markedly from that of Gd–DTPA which shows a maximum around 310 K (Figure 5). In the low-temperature range (276 to 310 K), $1/T_2^r$ of **L^3·Gd** is very low and nearly constant. Above 310 K, an increase of $1/T_2^r$ is observed, in agreement with a slow-exchange regime. The theoretical adjustment of the experimental data, performed as previously described,[59–61] allows, in principle, for the determination of the following parameters: $A/\hbar$, the hyperfine coupling constant between the oxygen nucleus of bound water molecules and the Gd^{3+} ion; τ_V, the correlation time modulating the electronic relaxation of Gd^{3+}; E_v, the activation energy related to τ_V; B, related to the mean-square of the zero-field-splitting energy Δ ($B = 2.4\Delta^2$); and $\Delta H^‡$ and $\Delta S^‡$ the enthalpy and entropy of activation of the water exchange process (Table 3).

The analysis of the experimental data (between 320 and 354 K) by the appropriate theoretical model provides a residence time of the coordinated water molecule (τ_M) of 3.5 μs at 310 K and 5.2 μs at 298 K. The value at 310 K is 25 times larger than that obtained for Gd–DTPA (143 ns). Consequently, the proton relaxivity at 310 K should be limited by the water residence time. It has been reported in several studies on Gd–DOTA and Gd–DTPA derivatives that the steric crowding around the lanthanide ion could play a role in the water exchange rate: less crowding means a longer the water residence time.[3d,10b,10c,19b,59–62] Since the distances between the lanthanide ion and the coordinating oxygen atoms are usually shorter than with the coordinating nitrogens, the complex studied in this work characterized

(54) Werts, M. H. V.; Verhoeven, J. W.; Hofstraat, J. W. *J. Chem. Soc., Perkin Trans. 2* **2000**, 433–439.
(55) Solomon, I. *Phys. Rev.* **1955,** *99*, 559–565.
(56) Bloembergen, N. *J. Chem. Phys.* **1957**, *27*, 572–573.
(57) Freed, J. H. *J. Chem. Phys.* **1978**, *68*, 4034–4037.
(58) Aime, S.; Botta, M.; Fedeli, F.; Gianolio, E.; Terreno, E.; Anelli, P. *Chem.–Eur. J.* **2001**, *7*, 5262–5269.
(59) Vander Elst, L.; Maton, F.; Laurent, S.; Seghi, F.; Chapelle, F.; Muller, R. N. *Magn. Reson. Med.* **1997**, *38*, 604–614.
(60) Laurent, S.; Vander Elst, L.; Houzé, S.; Guérit, N.; Muller, R. N. *Helv. Chim. Acta* **2000**, *83*, 394–406.
(61) Laurent, S.; Botteman, F.; Vander Elst, L.; Muller, R. N. *Magn. Reson. Mater. Phys. Biol. Med.* **2004**, *16*, 235–245.
(62) Powell, D. H.; Ni Dhubhghaill, O. M.; Pubanz, D.; Helm, L.; Lebedev, Y. S.; Schlaepfer, W.; Merbach, A. E. *J. Am. Chem. Soc.* **1996**, *118*, 9333–9346.

Table 3. Parameters Obtained for Complex by the Theoretical Adjustment of the ^{17}O Transverse-Relaxation Rate

	τ_M^{310} (ns)	$\Delta H^{\ddagger}$ (kJ mol^{-1})	$\Delta S^{\ddagger}$ (J mol^{-1} K^{-1})	$A/\hbar$ (10^6 rad s^{-1})	B (10^{20} s^{-2})	τ_V^{298} (ps)	E_v (kJ mol^{-1})
L^3·Gd	3471 ± 523	22.2 ± 0.2	−68.9 ±0.6	−4.5 ± 1.2	0.10 ±7.4	98 ± 95	1.9 ± 14.0
Gd-DTPA	143 ± 25	51.5 ± 0.3	52.1 ± 0.6	−3.4 ± 0.1	2.60 ± 0.06	12.3 ± 0.3	4.52 ± 4.22

by 5 nitrogen- and 3 carboxylic oxygen-coordinating atoms should be less crowded than Gd−DOTA (4 nitrogen- and 4 oxygen-coordinating atoms) or Gd−DTPA (3 nitrogen- and 5 oxygen-coordinating atoms). Additionally, the bipyridine structure reduces the flexibility of the ligand backbone, this could result in an increased distance between the two pyridinic nitrogen atoms and the Gd ion and therefore lead to a lower steric hindrance.

The errors on the parameters related to the relaxation time of the bound nuclei are very large since, in the temperature range investigated, only the slow exchange regime is observed. The water residence time is thus well defined, whereas the fitted parameters, $A/\hbar$, τ_V, E_v, and B should be considered to be rough estimations.

The evolution of the proton longitudinal relaxivity at 20 MHz at various temperatures (Figure 6) confirms that the exchange of the water molecule is very slow since no significant change is observed between 30 °C and 75 °C and a slight increase of the relaxivity is observed at low temperatures where the outer-sphere relaxivity is expected to be largely predominant. Water molecules in a second hydration sphere could also contribute to this increase.

Proton NMRD Profiles. The influences of the temperature and of the concentration on the proton NMRD profiles have been studied (Figure 7 and Supporting Information Figure S7). At 310 K, no significant influence of the concentration was recorded and as expected from the slow water exchange, the relaxivity at low, medium, and high fields is only slightly affected by the temperature change between 37 °C and 75 °C, but at lower temperatures, a slight increase of r_1 is observed at all fields. The proton relaxivity at 20 MHz is larger than expected taking into account the size and the water exchange rate (3.4 s^{-1} mM^{-1} at 310 K) and is comparable to that of Gd−DTPA. The presence of water molecules in a second sphere and in rapid exchange with the solvent could explain this phenomenon.

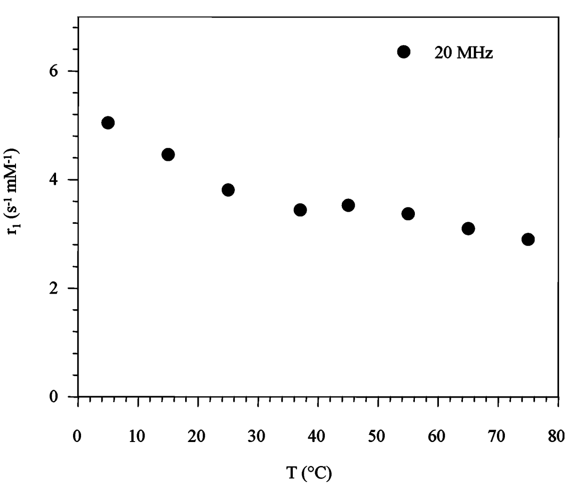

Figure 6. Temperature dependence of the proton longitudinal relaxivity of **L^3·Gd** complex (between 5 °C and 75 °C and at 20 MHz).

Table 4. Relative Diffusion Coefficient and Values of τ_M, τ_R, τ_{SO}, τ_V, and τ_{SS} Obtained from the Theoretical Fitting of the Proton NMRD Profiles

	D (10^{-9} m^2 s^{-1})^a	τ_M (μs)^b	τ_R (ps)	τ_{SO} (ps)	τ_V (ps)	τ_{SS} (ps)
5 °C^c	1.43	10.5	293	226	15	−
			180	120	18	69.9
15 °C^c	1.97	7.22	193	227	11	−
			110	128	18.4	45.9
25 °C^c	2.49	5.11	98	213	9	−
			75.0	123	15.1	36.1
37 °C^c	3.3	3.47	73	244	10	−
			57.2	120	11.7	32.4
45 °C^c	3.96	2.72	72	252	7	−
			57.0	138	12.5	26.8
55 °C^c	4.84	2.04	62	283	21	−
			50.0	175	19.4	21.2
65 °C^c	5.75	1.56	52	338	17	−
			43.5	200	14.0	19.0
75 °C^c	6.7	1.21	44	404	35	−
			36.7	220	15.0	17.8

^{a} The relative diffusion coefficient is the coefficient of pure water × 1.1. ^{b} Value obtained from ^{17}O NMR spectroscopy. ^{c} The first line corresponds to the data obtained by the first fitting (inner-sphere and outer-sphere contributions), whereas the second line corresponds to the data obtained by the second fitting (inner-sphere, outer-sphere and second-sphere contributions).

The theoretical analysis of the NMRD profiles (Table 4) has thus been performed either with the usual inner-sphere and outer-sphere contributions or with three contributions: inner-sphere, outer-sphere, and second-sphere. Some parameters were fixed: the number of water molecules in the first coordination sphere, q, was set to the value obtained by luminescence data ($q = 1$), the distance of closest approach, d ($d = 0.36$ nm in the first fitting and 0.45 nm in the second one), the relative diffusion coefficient D ($D = 1.1 \times$ the diffusion coefficient of water at the same temperature), the distance between the proton nuclei of the bound water and the gadolinium ion, r ($r = 0.31$ nm), the water residence

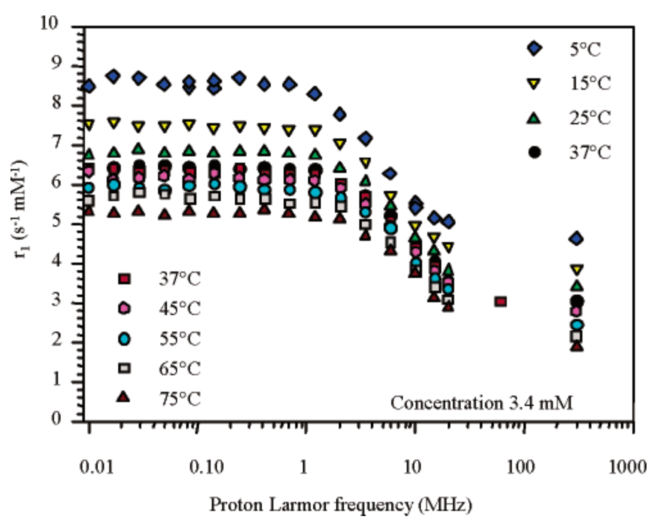

Figure 7. ^{1}H NMRD relaxivity profiles of **L^3·Gd** complex in water at different temperatures.

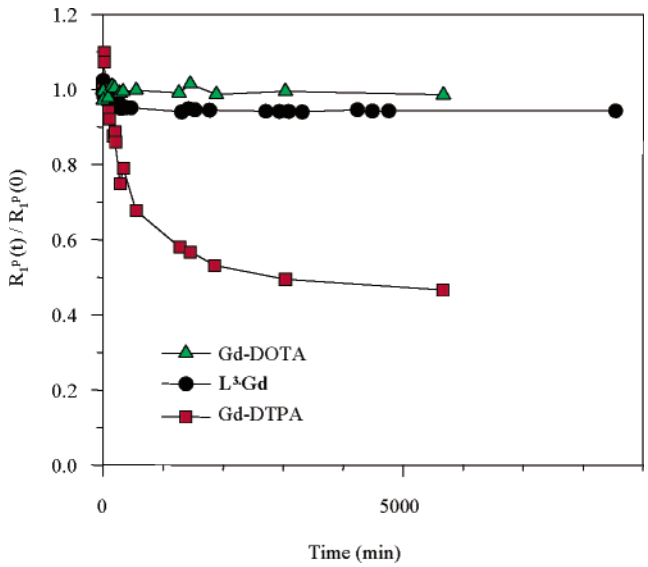

Figure 8. Evolution of the ratio $R_1^p(t)/R_1^p(0)$ as a function of time during transmetalation experiment.

time, $\tau_{M,}$ was fixed to the value determined by ^{17}O relaxometry, and the distance for the second-sphere interaction, r_{SS} ($r_{SS} = 0.4$ nm). The parameters describing the rotational correlation time, τ_R, the electronic relaxation times, τ_V and τ_{SO} (the electronic relaxation time at zero field) and the correlation time for the second sphere molecules τ_{SS} ($\tau_{SS}^{-1} = \tau_R^{-1} + \tau_{MSS}^{-1}$), were optimized simultaneously. The first theoretical adjustment results in quite large values of τ_{SO} at all temperatures and of τ_R at low temperatures (5 and 15 °C), and there is a poor agreement between the measured and fitted data at 300 MHz for the two lower temperatures (Figure S8 Supporting Information). At higher temperatures, the agreement between the experimental data and fitted values is better. The second theoretical adjustment gives three water molecules in the second sphere and a better agreement between the observed and fitted data. Both adjustments obtained at 5, 25, 37, and 75 °C are shown in Supporting Information (Figure S8). The latter τ_R values are in the same range as those of gadolinium complexes of similar size,[60] and a value of 16.7 kJ/mol can be calculated for the activation energy related to the rotation (E_R). This value agrees quite well with those reported for Gd−DTPA, Gd−DTPABMA, or Gd−DOTA.[62] Moreover, the τ_{SO} values are closer to the values reported for the Gd−DTPA derivatives.

Transmetalation by Zn^{2+} Ions. Transmetalation of the Gd complex by Zn^{2+} results in the release of gadolinium ions in solution. In the presence of phosphate ions, Gd ions precipitate and no longer contribute to the proton paramagnetic-relaxation rate of the solution.[30] Consequently, the water proton-relaxation rate decreases, and its evolution can be used to quantitatively monitor the evolution of the system. No significant change of the paramagnetic relaxation rate was noticed for the **L³·Gd**. This stability can be compared to that of the macrocyclic gadolinium complexes Gd−DOTA. On the contrary, R_1^p decreased to about 50% of its initial value for Gd−DTPA after 5000 minutes, showing that a significant transmetalation occurs (Figure 8). The present results confirm the data obtained on the europium complex (see above).

Interaction with Human Serum Albumin. The paramagnetic-relaxation rate of solutions containing 1 mM complex in water or in 4% HSA are quite similar at 0.47 T and 310 K (R_1^p(HSA)/R_1^p(water) = 1.3). If there was a significant interaction between the complex and HSA, the complex bound to HSA would experience a much slower rotational mobility and its relaxation rate would significantly increase. Hence, a marked increase of the paramagnetic relaxation rate would be expected at this magnetic field. It seems thus that a significant interaction of **L³·Gd** with the protein can be excluded in good agreement with the data obtained for the europium complex (vide supra).

Conclusions

We have synthesized a novel macrocyclic octadentate ligand, based on 2,2′-bipyridine and a diethylenetriaminetriacetic core. The resulting 1:1 lanthanide complexes display excellent thermodynamic stability (K_{cond}(Eu) > 10^{18} at pH 7.4) and kinetic stability versus demetalation by blood proteins and transmetalation by several bioactive cations. They could thus be used safely in vivo. Coordination features revealed that one water molecule is present in the first coordination sphere of the metal, allowing us to investigate the luminescence and relaxivity properties of these complexes. Investigations of the photophysical properties establish that bipyridine unit acts as an efficient energy-transferring antenna in these complexes. Upon excitation into the ligand-centered absorption bands, large quantum yields were obtained for Eu(III) and Tb(III) in air-equilibrated water solutions at room temperature ($\Phi = 0.10$ and 0.21, respectively). This luminescence is little affected by the temperature, showing that back-energy transfer from the metal-emitting state to the bipyridine lowest triplet state or population of the upper-lying excited states of other configurations (particularly LMCT states) do not play a significant role in these systems. The ligand **L^3H_3** also sensitizes the luminescence of Sm(III) and Dy(III) ions, although the small energy gap between the luminescent state and the highest J level of the ground state of these ions contributes to their weaker luminescence. The potential use of **L³·Gd** as an MRI contrast agent was evaluated by measuring in vitro the water proton-relaxation enhancement. The relaxivity, r_1 (20 MHz, 310K), of this complex is 3.4 s^{-1} mM^{-1}, similar to that of the Gd−DTPA complex ($r_1 = 3.9$ s^{-1} mM^{-1}),[10c] which is currently used in clinical applications on a routine basis. This relaxivity is not or only slightly affected by concentration or temperature changes. On the other hand, ^{17}O NMR and ^1H NMRD experiments suggest that the limiting factor for the relaxivity of the **L³·Gd** complex is the slow exchange rate of the coordinated water molecule ($\tau_M = 3.5$ μs). However, a contribution of a second-sphere interaction could explain the observed relaxivity. Some structural modifications allowing a decrease in the residence lifetime of the bound water molecule could thus be beneficial for this type of complex. This work is in progress.

Acknowledgment. This work was supported by the CNRS and the Ministry of Research of France. F.H. thanks the CNRS for a postdoctoral fellowship. S.L., L.V.E., and R.N.M. thank the ARC Program 00/05-258 of the French Community of Belgium and kindly acknowledge the support and sponsorship of COST Action D18 "Lanthanide Chemistry for Diagnosis and Therapy". Dr J. M. Couchet is gratefully acknowledged for the separation and characterization of compounds **6·Na** and **6**.

Supporting Information Available: ^{1}H NMR spectra of **6·Na** and **L^3H_3**, MS spectra and titration experiments for **L^3·Eu**, electronic level diagram for the **L^3·Gd** complex and lanthanide ions, UV−vis absorption and excitation spectra of **L^3·Sm**, effects of added cations, anions, and BSA on the luminescence data of **L^3·Eu**, ^{1}H NMRD relaxivity profiles of **L^3·Gd** at various concentrations and theoretical fittings. This material is available free of charge via the Internet at http://pubs.acs.org.

IC0507722